



Photocatalytic and optical properties of NiO added *Nephelium lappaceum L.* peel extract: An attempt to convert waste to a valuable product



T. Adinaveen^{a,b,*}, Thenmozhi Karnan^c, Stanly Arul Samuel Selvakumar^d

^a Department of Chemistry, Madras Christian College, Chennai 600 059, India

^b Department of Chemistry, Loyola College, Chennai 600 034, India

^c Department of Chemistry, University College of Engineering, Kanchipuram 631 552, India

^d Department of Applied Chemistry, Sri Venkateshwara College of Engineering, Sriperumpudur, Tamil Nadu 602 117, India

ARTICLE INFO

Keywords:

Environmental science
Nanotechnology
Natural product chemistry
Materials chemistry

ABSTRACT

In our present study, we have reported the fabrication of a simple, low-cost and ultra-violet active Nickel oxide Substituted *Nephelium lappaceum L.* peel extract photocatalyst. The synthesized photocatalyst samples were characterized by a combination of various physicochemical techniques. The degradation of Rhodamin b (RhB) shows excellent durability and recyclability properties. The remarkable enhancement in photoactivity under ultra-violet light irradiation can be attributed to the decrease in band gap by plant extract substitution. In our investigation, we report for the first time the synthesized NiO NPs using Rambutan (*Nephelium lappaceum L.*) undergo photocatalytic activity studies against cationic dye, Rhodamin b under UV light illumination. The result shows that the NiO NPs shows high degradation activity against RhB (92.3%). A plausible mechanism for the formation of NiO NPs from the biological source was also proposed. The outcome of the present study is an effective approach to design environmental friendly material for treating dyeing industry effluent.

1. Introduction

Nowadays, the need for designing eco friendly synthetic protocols for nanoparticle synthesis leads to increasing the interest in 'Green nanotechnology'. The term 'green' indicates that the technology is environmentally benign and sustainable; the technology is proposed to contribute to the solution of environmental problems associated with the fabrication of nano based materials [1, 2]. Green chemistry principles drive researchers to develop nanoparticles via microorganisms and plant extracts. But, the use of plant sources in the form of extracts has emerged as an efficient synthetic route compared to other biological entities because it does not require any special, complex, multistep procedures like culture preparation, isolation and culture maintenance and incorporates support for large scale synthesis of nanoparticles [3, 4, 5]. In addition, it comprises easy availability, low cost, green approach, simpler down streaming processing etc. [6].

Naturally available plant materials have the high potential to fabricate micro and nano scaled inorganic materials namely magnetic, metallic and metal oxide materials. Recently, there is an emerging interest in biologically synthesizing metal oxide nanoparticles like ZnO [7], CuO [8], Fe₂O₃ [9], Bi₂O₃ [10] and CeO₂ [11] etc due to their distinct

properties and potential uses in diverse fields including chemical sensors, field effect transistors, catalyst, drug delivery agents, electronics, optics and magnetic storage devices. At present, very few literatures are available on the green synthesis method of NiO as compared to other methods. That is the reason to select NiO nanoparticles in this study.

Generally, Nickel oxide is a rock salt structure with typical antiferromagnetic nature at 523 K [12]. The most important features of NiO are excellent electrochemical stability, low cost, durability and a good ion storage material with large span optical density [13, 14, 15, 16].

Though several methods are used to prepare NiO NPs, green synthesis method will be more significant and enduring approaches towards environmental benign route. In this case, Rambutan fruit peel is selected as a biological entity for the preparation of NiO NPs. Rambutan (*Nephelium lappaceum L.*) is a variety of popular tropical fruit which belongs to Sapindaceae family related to the longan and lychee, originated from Southeast Asia. Corilagin, geranin, ellagic acid, and ellagitannins are the primary polyphenolic components present in rambutan [17]. The probable mechanism of formation of NiO NPs was given in Fig. 1. Ellagic acid acts as a ligation agent. The hydroxyl groups present in ellagic acid ligate with metal ions and forming metal-ellagate complex by chelating effect. It may be owing to the rambutan extracts which acquire

* Corresponding author.

E-mail address: adinavee@gmail.com (T. Adinaveen).

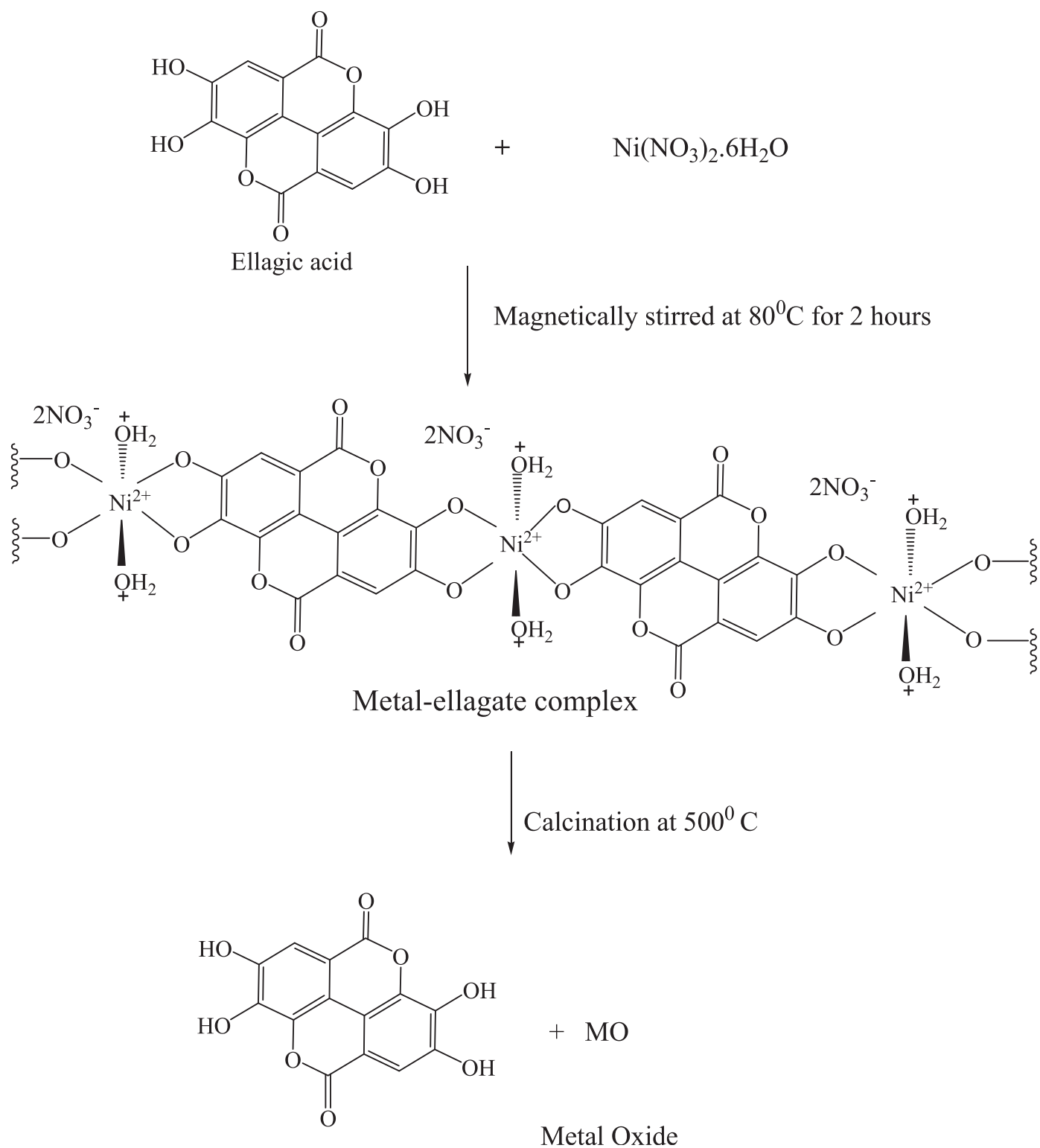


Fig. 1. Possible formation scheme of NiO Nps using rambutan fruit peel extract.

ellagic acid which actively attracts the cations and triggers NiO NPs synthesis. In addition, all these factors accumulatively support the synthesis of bioinspired NiO NPs in the presence of rambutan peel extract. These results show that, the presence of rambutan ellagic acid appears to attach the surface of the bioinspired NiO NPs nanoparticles. Previously, such behavior has been observed in the presence of ellagic acid [18]. Then, this complex undergoes hydrolysis process to precipitate metal ions as metal hydroxides or metal oxides

depending upon the reaction conditions like pH. Nickel-ellagate complex finally subjected to decomposition under calcinations at 500°C to yield NiO nanoparticles [19]. NiO NPs was prepared already using Rambutan and reported their antibacterial activity [14]. In this study, for the first time, we have reported the photocatalytic activity of NiO NPs using Rambutan (*Nephelium lappaceum L.*) against Rhodamin b under UV light illumination.

2. Materials and methods

2.1. Materials

The *Nephtelium lappaceum* L. was purchased from fruit market at Kanchipuram, India. Nickel nitrate [Ni (NO₃)₂.6H₂O], ethanol along with RhB were purchased from Merck chemicals Ltd., and used as purchased. Deionised water was used for the preparation of samples.

2.2. Preparation of the extract

Fresh peels of *Nephtelium lappaceum* L. were washed carefully with water and then cut into pieces and undergo shaded drying in open environment. The dried *Nephtelium lappaceum* L. peels were boiled with double distilled water (40 ml) and ethanol (20 ml) in 2:1 ratio for 15 min for complete extraction. 60 °C was the temperature maintained during extraction. The obtained extract was filtered using Whatman No. 1 filter paper and the resultant filtrate was collected in container and stored in electric refrigerator for further use [14].

2.3. Green synthesis of nickel oxide nanoparticles

An aqueous solution of 0.1 M nickel nitrate [Ni (NO₃)₂.6H₂O] was prepared with 50 ml deionised water. To this, 10 ml of *Nephtelium lappaceum* L. extract was added and stirred at 80 °C for 2 h. The particles were collected by centrifugation at 8000 rpm for 15 minutes. Later on, the collected particles were washed thoroughly with deionised water and centrifuged at 5000 rpm for 10 minutes. The resulting sample was dried and powdered. Then the sample was calcined in a heating furnace at 500 °C for 2 h to obtain pure NiO NPs.

2.4. Instrumentation

X-ray diffractometer (JEOL IDX 8030 instrument operating at 40 kV) was used to study the crystalline morphology in the sample. The surface morphology was studied using field emission scanning electron microscope (FESEM-SUPRA 55) and transmission electron microscope (TEM) (JEOL JEM 3010). X-ray photoelectron spectra (XPS) were measured using Physical Electronics Model 5400 spectrometer. The optical properties were studied using diffuse reflectance spectrophotometer (DRS) Shimadzu (UV 2450) UV-VIS instrument using BaSO₄ as standard with the wavelength range of 200–800 nm. Micromeritics ASAP 2400 surface area analyser was used to measure the surface area. Degradation of RhB solution was recorded using UV-Visible spectrophotometer (SHIMADZU UV-1650 PC).

2.5. Photocatalytic studies

Rhodamine B (RhB) is an industrial dye used as a base material for this study. It is highly carcinogenic and causes redness, irritation and pain in the skin and eyes. If swallowed, RhB is will cause irritation to the gastrointestinal tract. Therefore, it is very important to remove RhB from the waste before discharging to nature [20].

The photocatalytic degradation of cationic dye RhB was carried out at room temperature. A Heber Multi lamp photoreactor (HML MP 88 light source with 8 W) power and medium pressure mercury vapour lamps was used. A total of 100 mg of NiO NPs was loaded into 100 ml of simulating pollutant such as RhB (1×10^{-5} mol/L, 10 ppm) to achieve a concentration of 1 mg ml⁻¹. The suspension was stirred for uniform mixing. For every photocatalytic degradation, the overall quantity of photocatalyst was same. Before illumination of UV radiation, the reaction suspension undergo magnetic stirring for 45 minutes in order to adsorption-desorption equilibrium between catalyst and the simulate pollutant. 3 mL aliquots were sampled and centrifuged at 6000 rpm for 20 min at frequent time intervals. Then the supernatants were analyzed the absorbance at 554 nm by using UV-Vis spectrophotometer. Finally,

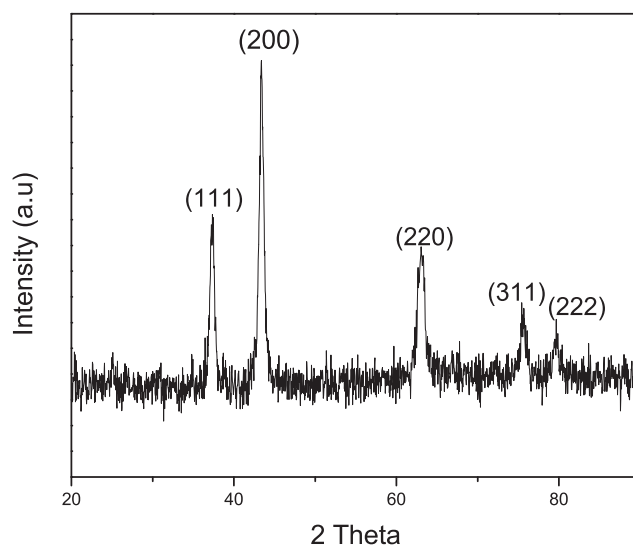


Fig. 2. XRD pattern of biosynthesized NiO Nps calcined at 500°.

the photocatalytic degradation efficiency (PDE) percentage was calculated using the formula,

$$\text{PDE (\%)} = \frac{(\text{Absorbance})_0 - (\text{Absorbance})_t}{(\text{Absorbance})_0} \times 100 \quad (1)$$

Where (Absorbance)₀ is the absorbance before irradiation and (Absorbance)_t is the absorbance at time t. The mineralization was calculated using a COD (Chemical Oxygen Demand) value which was calculated for analyzing complete decomposition of organic compound into carbon dioxide, water and other inorganic minerals. The COD of dye solution was calculated for pre and post photocatalytic treatment using dichromate method.

3. Results and discussion

3.1. XRD patterns

Fig. 2 shows the X-ray diffraction pattern of obtained NiO NPs. The recorded diffraction peaks appeared at $2\theta = 43.28^\circ, 37.25^\circ, 62.87^\circ, 75.41^\circ$ and 79.40° which are well indexed to the (2, 0, 0), (1, 1, 1), (2, 2, 0), (3, 1, 1) and (2, 2, 2) crystal planes of NiO. All the recorded peaks in the patterns were well indexed to face centered cubic (FCC) structured NiO with lattice parameters of $a = 0.4177$ nm, which were very close to the standard data of JCPDS (Joint Committee on Powder Diffraction Standards) file No. 78-0429 [21]. Moreover, there were no other peaks present, suggesting that all the intermediates completely converted into product. The crystallite size was calculated from the major diffraction peaks, i.e (2, 0, 0) of NiO using Debye-Scherrer formula, $D = 0.94\lambda/\beta \cos \theta$. Where D is the crystallite size in nanometers, 0.94 is the dimensionless constant k , β is the half-height width of the diffraction peak, θ is the diffraction angle, and λ is the X-ray wavelength (0.1541 nm). The crystallite size of NiO NPs was found to be 19.6 nm.

3.2. FE-SEM analysis

The FE-SEM image of biosynthesized NiO NPs was shown in Fig. 3 (a-b). It can be seen from the image that the NiO NPs possess homogeneous spherical like structure and the particles are in monodispersing nature. The shape of the NiO NPs particles is basically globular and the particle diameters are in the range of 15–20 nm. The size of NiO NPs obtained from the X-ray diffraction studies are in good agreement with the SEM studies [22]. The SEM images shows that the particles are spherical with homogeneous agglomeration to give large crystals, which may be by

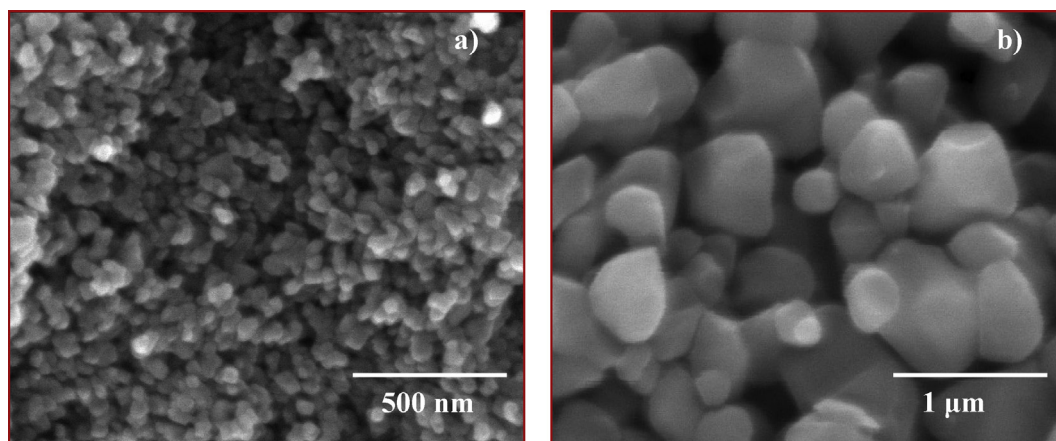


Fig. 3. FE-SEM image of (a) and (b) biosynthesized NiO NPs at different magnification.

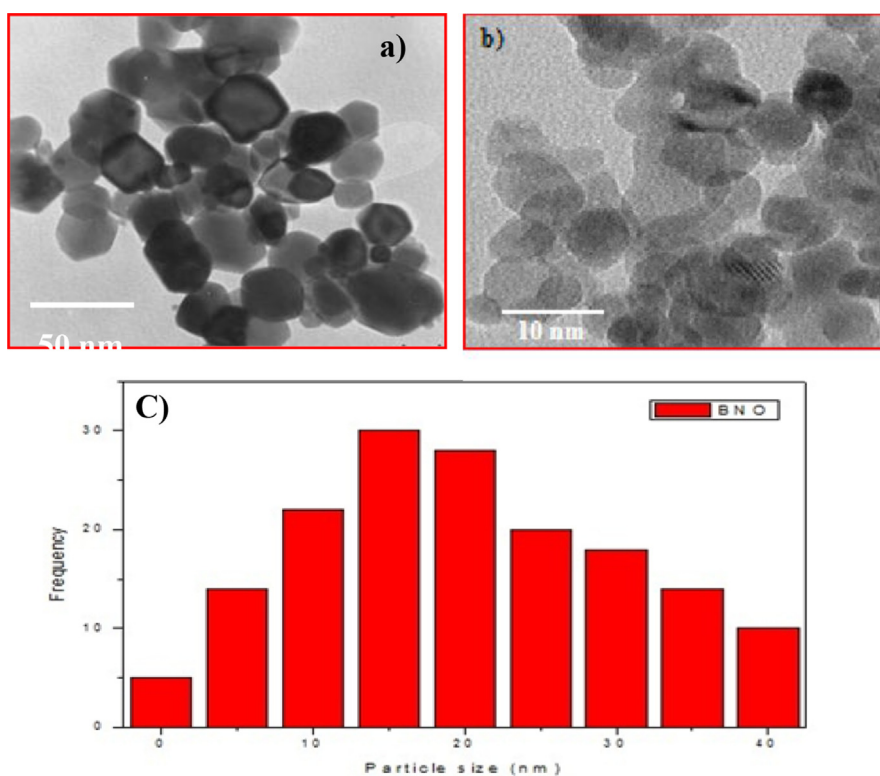


Fig. 4. HR-TEM images of (a) and (b) biosynthesized NiO NPs at different magnification (c) particle size distribution histogram of NPs.

reason of the preparation method, defects and the effect of annealing temperature. It is a recognized fact that the reaction time and temperature are the two essential factors in influencing the morphology of the nanomaterials. Aggregation of particles is not apparent in the case of NiO NPs. The uniform morphology leads to high photocatalytic behaviour.

3.3. HR-TEM analysis

The HR-TEM images of NiO NPs with different magnifications have been shown in Fig. 3 (a) and (b). Fig. 4 (c) shows the particle size distribution histogram of NPs. The TEM images show the morphology of NiO NPs. The image indicates that the nanoparticles had spherical shape and are self assembled. The TEM image at 50 nm and 10 nm clearly shows that the particles are equally distributed except for few aggregated particles. In addition, the BET (Brunauer-Emmett-Teller) surface area of NiO NPs was found to be 67.76 m²/g. This may lead to enhance the

photocatalytic studies since large surface area having more reactive sites for further reaction.

3.4. Elemental analysis

The chemical composition of the synthesized sample was analyzed with the help of EDS (Energy dispersive spectroscopy) analysis and the result showed in Fig. 5. This spectrum confirms the existence of Ni and O elements and there were no other impurities. The weight percentage observed from energy dispersive spectra was given as table in inset of image. This table reveals that the formed nanoparticles are rich in nickel content compared to oxygen.

3.5. X-ray photoelectron spectra analysis

Fig. 6 Shows the X-ray photoelectron spectra (XPS) of NiO NPs. The

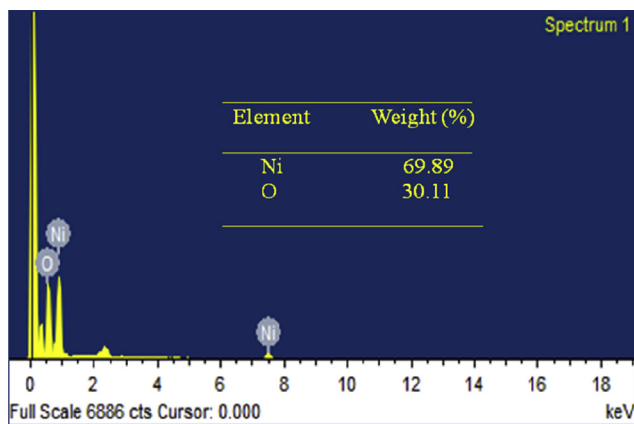


Fig. 5. EDS spectrum of NiO Nps with quantitative results as inset.

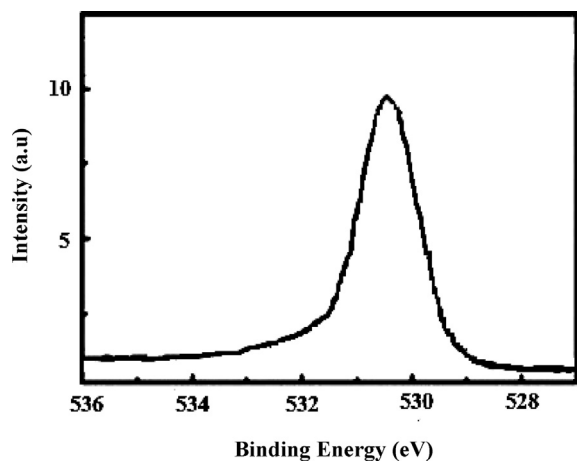


Fig. 6. XPS spectra of the sample NiO Nps.

peak at 530.5 eV corresponds to NiO NPs [23]. This spectrum proves the existence of NiO NPs and there were no other impurities observed in the spectra further confirm the purity of the as prepared sample. This result was in good agreement with the result observed in EDS spectra, which suggests the possibility of this ellagic acid acting as a good ligation agent that would be associated with the formation of NiO NPs [24].

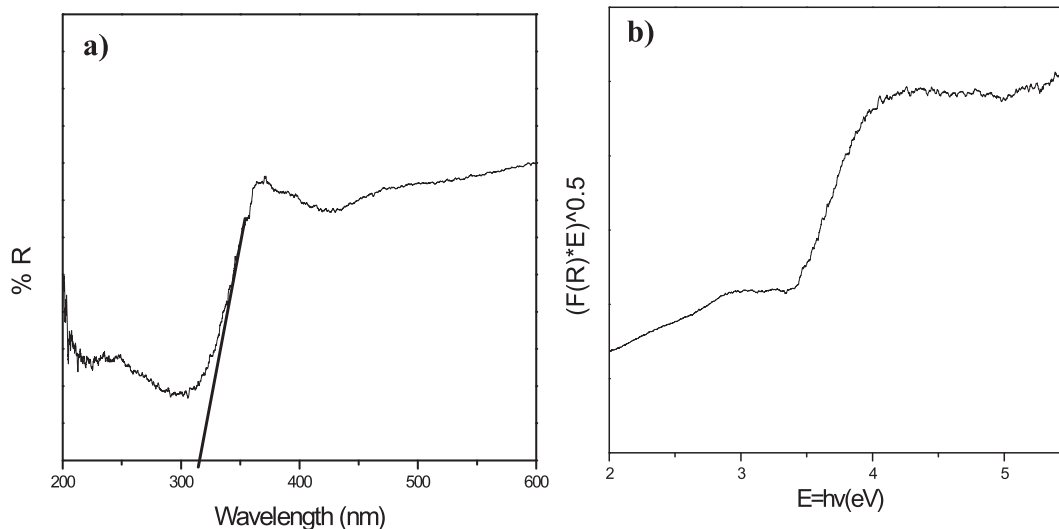


Fig. 7. a) UV-Visible diffuse reflectance spectroscopy of the sample NiO Nps, b) shows the band gap energy of NiO NPs calculated using KubelkaMunk function using the reflectance data of the absorption coefficient.

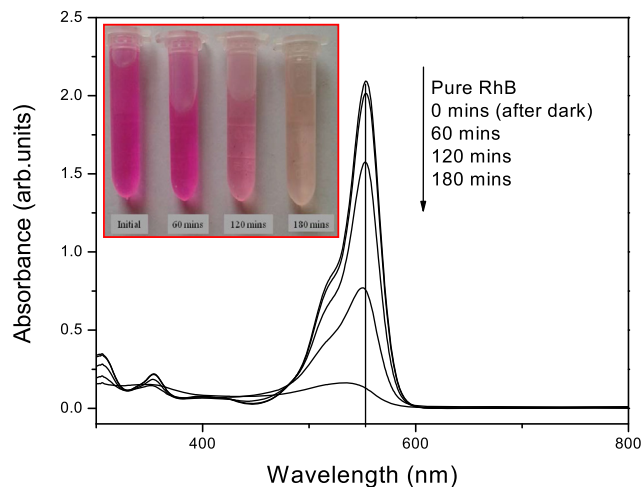


Fig. 8. Time dependent UV-Visible spectra of RhB dye in aqueous dispersion of NiO Nps and the insert figure shows the decolorisation of the dye from strong pink to colorless.

3.6. UV-visible DRS studies

The optical property of the fabricated NiO NPs was studied by using UV-Visible diffuse reflectance spectroscopy, which was shown in Fig. 7a. It could be seen from the figure that, their absorption edges are located around 319 nm for nickel oxide nanoparticles. This means that, the wavelength shows the photoresponse in the range of UV light. Similar result of absorption wavelength has been reported earlier [25]. Fig. 7b shows the band gap energy of NiO NPs calculated using Kubelka-Munk function using the reflectance data of the absorption coefficient. The optical band gap (E_g) was calculated by using the formula,

$$\text{Band Gap } (E_g) = \frac{1240}{\text{Wavelength (nm)}} \quad (2)$$

Based on the formula, the calculated band gap of NiO NPs was found to be 3.8 eV.

3.7. UV spectral analysis

UV-Visible spectrum was recorded during photodegradation of RhB (Rhodamin B) using NiO NPs was shown in Fig. 8. RhB absorbs the light

Table 1
Comparison of photocatalytic activity of NiO NPs with different photocatalysts.

Materials Used	Biological Entity	Pollutant	Degradation efficiency (%)	Degradation time (min)	References
NiO	<i>Nepheleium lappaceum L</i>	Rhodamin B	92.3	180	Present work
ZnO	<i>Nepheleium lappaceum L</i>	Methyl orange	83.99	120	[7]
TiO ₂	<i>Jatropha curcas L</i>	Tannery wastewater	82.26	300	[26]
ZnO	<i>Pyrus pyrifolia</i>	Methylene blue	80.3	210	[27]
ZrO ₂	<i>Ficus benghalensis</i>	Methyl orange	69	240	[28]

in the maximum range at 554 nm. The synthesized NiO NPs exhibit high photocatalytic activity for decomposition RhB dye under UV light and the photocatalytic degradation ratio of RhB attains 92.3% after illumination of 180 mins. For the purpose of comparison, dark experiment also carried out and the result reveals only less than 2% degradation obtained. We have compared the photocatalytic catalytic activity NiO NPs with other photocatalysts and tabulated the results as Table 1. The absorption band of RhB shifted from 554 nm to 537 nm shows the removal of ethyl groups during irradiation. In addition, the color of the reaction suspension also changes owing to destruction of chromophoric group from the dye, which is shown as insert of Fig. 8. In this figure, the decolorisation visually proved by gradual change in color of the dye from strong pink to colorless.

3.7. Mineralization studies

A Minaraliation study was done with the help of COD measurement. Here, organic compound converted into water, carbon dioxide and other inorganic ions. The mineralization efficiency of RhB dye was reported by measuring initial and final COD value under UV light. Noticeably, the COD value of RhB dye after illumination of 180 mins indicates 64.7% mineralization.

4. Conclusion

Green synthesis method is a best alternate method to prepare NiO NPs s. The prepared nanoparticles was nearly spherical, has a surface area 67.76 m²/g and the crystallite size 19.6 nm The synthesized NiO NPs is an active photocatalyst for Rhodamin B degradation under UV light. The COD value of RhB dye after illumination shows 64.7% mineralization. The outcome of the present study is an effective approach to design environmental friendly material for treating dying industry effluent.

Declarations

Author contribution statement

T. Adinaveen: Conceived and designed the experiments; Wrote the paper.

Thenmozhi Karnan: Performed the experiments; Contributed reagents, materials, analysis tools or data.

Stanly A. S. Selvakumar: Analyzed and interpreted the data; Contributed reagents, materials, analysis tools or data.

Funding statement

This research did not receive any specific grant from funding agencies in the public, commercial, or not-for-profit sectors.

Competing interest statement

The authors declare no conflict of interest.

Additional information

No additional information is available for this paper.

Acknowledgements

The authors are grateful to i) The Principal and Management, Madras Christian College, Chennai. ii) The Dean, University College of Engineering Kanchipuram and iii) The Principal and Management, Sri Venkateshwara College of Engineering, Sriperumpthur for their infrastructural support. Also, we thank the Coordinator, Science Instrumentation Center, SFR College for Women, Sivakasi for recording diffuse reflectance spectra.

References

- [1] Manuela Stan, Adriana Popa, Toloman Dana, Adriana Dehelean, Ildiko Lung, Katona Gabriel, Enhanced photocatalytic degradation properties of zinc oxide nanoparticles synthesized by using plant extracts, Mater. Sci. Semicond. Process. 39 (2015) 23–29.
- [2] Y. Abboud, T. Saffaj, A. Chagraoui, A. El Bouari, K. Brouzi, O. Tanane, B. Ihssane, Biosynthesis, characterization and antimicrobial activity of copper oxide nanoparticles (CONPs) produced using brown alga extract (*Bifurcaria bifurcata*), Appl. Nanosci. 4 (2014) 571–576.
- [3] Siavash Irvani, Green synthesis of metal nanoparticles using plants, Green Chem. 13 (2011) 2638–2650.
- [4] Mohd Sayeed Akhtar, Jitendra Panwar, Yeoung-Sang Yun, Biogenic synthesis of metallic nanoparticles by plant extracts, ACS Sustain. Chem. Eng. 1 (2013) 591–602.
- [5] Monaliben Shah, Derek Fawcett, Shashi Sharma, Suraj Kumar Tripathy, Gérrard Eddy Jai Poinern, Green synthesis of metallic nanoparticles via biological entities, Materials 8 (2015) 7278–7308.
- [6] Narendra Kulkarni, Uday Muddapur, Biosynthesis of metal nanoparticles: a review, J. Nanotechnol. (2014) 8. Article ID 510246.
- [7] Thenmozhi Karnan, Stanly Arul Samuel Selvakumar, Biosynthesis of ZnO nanoparticles using rambutan (*Nepheleium lappaceum L.*) peel extract and their photocatalytic activity on methyl orange dye, J. Mol. Struct. 1125 (2016) 358–365.
- [8] Renu Sankar, Perumal Manikandan, Viswanathan Malarvizhi, Tajudeennasrin Fathima, Kanchi Subramanian Shivashangari, Vilwanathan Ravikumar, Green synthesis of colloidal copper oxide nanoparticles using Carica papaya and its application in photocatalytic dye degradation, Spectrochim. Acta, Part A 121 (2014) 746–750.
- [9] Madhan Raja, Pearlin, Green synthesis of iron nanoparticles and investigation of their effect on degradation of dyes, J. Biol. Inform. Sci. 4 (2) (2015) 6–8.
- [10] Thenmozhi Karnan, StanlySamuel A novel bio- mimetic approach for the fabrication of Bi₂O₃ nanoflakes from rambutan(*Nepheleium lappaceum L.*) peel extract and their photocatalytic activity, Ceram. Int. 42 (2016) 4779–4787.
- [11] G. Sai Priya, Abhimanyu Kanneganti, K. Anil Kumar, K. Venkateswara Rao, Satish Bykkam, Bio synthesis of cerium oxide nanoparticles using Aloe barbadensis miller gel, IJSRP 4 (6) (2014) 1–4.
- [12] Victor V. Volkov, Z.L. Wang, B.S. Zou, Carrier recombination in clusters of NiO, Chem. Phys. Lett. 337 (2001) 117–124.
- [13] P.S. Patil, L.D. Kadam, Preparation and characterization of spray pyrolyzed nickel oxide (NiO) thin films, Appl. Surf. Sci. 199 (2002) 211–221.
- [14] R. Yuvakkumar, J. Suresh, A. JosephNathanael, M. Sundrarajan, S.I. Hong, Rambutan (*Nepheleium lappaceum L.*) peel extract assisted biomimetic synthesis of nickel oxide nanocrystals, Mater. Lett. 128 (2014) 170–174.
- [15] R. Manigandan, K. Giribabu, R. Suresh, S. Munusamy, S. Praveen kumar, S. Muthamizh, A. Stephen, V. Narayanan, Characterization and photocatalytic activity of nickel oxide nanoparticles, Int.J. ChemTech Res. 6 (6) (2014) 3395–3398.
- [16] M. Mohammadjoo, Z. Naderi Khorshidi, S.K. Sadrnezhad, V. Mazinani, Synthesis and characterization of nickel oxide nanoparticle with wide band gap energy prepared via thermochemical processing, Nanosci. Nanotechnol. An Int. J. (NLJ) 4 (1) (2014) 6–9.
- [17] Nont Thitilertdecha, Aphiwat Teerawutgulrag, Jeremy D. Kilburn, Nuansri Rakariyatham, Identification of major phenolic compounds from *Nepheleium lappaceum L.* and their antioxidant activities, Molecules 15 (2010) 1453–1465.
- [18] S.N. Barnaby, S.M. Yu, K.R. Fath, A. Tsiola, O. Khalpari, I.A. Banerjee, Ellagic acid promoted biomimetic synthesis of shape-controlled silver nanochains, Nanotechnology 22 (2011) 225605.
- [19] R. Yuvakkumar, J. Suresh, B. Saravanakumar, A. Joseph Nathanael, Ig Hong Sun, V. Rajendran, Rambutan peels promoted biomimetic synthesis of bioinspired zinc

- oxide nanochains for biomedical applications, *Spectrochim. Acta, Part A* 137 (2015) 250–258.
- [20] Fereshteh Motahari, Mohammad Reza Mozdianfard, Masoud Salavati-Niasari, Synthesis and adsorption studies of NiO nanoparticles in presence of H2acacen ligand, for removing rhodamine B in wastewater treatment, *Process Saf. Environ. Protect.* 93 (2015) 282–292.
- [21] Ravi Kant Sharma, Ranjana Ghose Synthesis of porous nanocrystalline NiO with hexagonal sheet-like morphology by homogeneous precipitation method, *Superlattice. Microst.* 80 (2015) 169–180.
- [22] M.S. Niasari, F. Davar, Z. Fereshteh, Synthesis of nickel and nickel oxide nanoparticles via heat-treatment of simple octanoate precursor, *J. Alloy. Compd* 494 (2010) 410–414.
- [23] P. Song, D. Wen, Z. Guo, T. Korakianitis, Oxidation investigation of nickel nanoparticles, *Phys. Chem. Chem. Phys.* 10 (2008) 5057–5065.
- [24] V. Bansal, A. Ahamad, M. Sastry, Fungus-mediated biotransformation of amorphous silica in rice husk to nanocrystalline silica, *J. Am. Chem. Soc.* 128 (2006) 14059–14066.
- [25] K. Anandan, V. Rajendran, Effects of Mn on the magnetic and optical properties and photocatalytic activities of NiO nanoparticles synthesized via the simple precipitation process, *Mater. Sci. Eng., B* 199 (2015) 48–56.
- [26] Surya Pratap Goutam, Gaurav Saxena, Varunika Singh, Anil Kumar Yadav, Ram Naresh Bharagava, Khem B. Thapa, Green synthesis of TiO₂ nanoparticles using leaf extracts of *Jatropha curcas* L. for photocatalytic degradation of tannery wastewater, *Chem. Eng. J.* 336 (2018) 386–396.
- [27] C. Parthiban, N. Sundaramurthy, Biosynthesis, characterization of ZnO nanoparticles by using *pyrus pyrifolia* leaf extract and their photocatalytic activity, *Int. J. Innov. Res. Sci. Eng. Technol* 4 (10) (2015) 9710–9718.
- [28] H.M. Shinde, T.T. Bhosale¹, N.L. Gavade, S.B. Babar, R.J. Kamble, B.S. Shirke, K.M. Garadkar, Biosynthesis of ZrO₂ nanoparticles from *Ficus benghalensis* leaf extract for photocatalytic activity, *J. Mater. Sci. Mater. Electron.* 29 (2018) 14055–14064.